2019 SECED Conference
Earthquake risk and engineering towards a resilient world
9-10 September 2019, Greenwich, London

REHABILITATION OF 20TH CENTURY CONCRETE HERITAGE BUILDINGS: THE CASE STUDY OF THE MUNICIPAL MARKET IN NICOSIA, CYPRUS

Antroula GEORGIOU[1], Ioannis IOANNOU[2] & Stavroula PANTAZOPOULOU[3]

Abstract: *Even though restoration norms for normal concrete and masonry structures are prescribed in existing international codes, the rehabilitation, conservation and protection of 20th century concrete heritage buildings is still a major challenge. The remarkable architectural, material and technological variety of these buildings and the lack of recognition of their cultural and historical value has often led to their abandonment and irreparable damage through the adoption of poor conservation practices. This research focuses on a representative case study of an early concrete building (Old Municipal Market) in Nicosia, Cyprus. The building is considered a typical example of Modern Architectural Heritage, with important social history and use. The study aims at the selection of appropriate techniques for the collection of data, simulation, evaluation and testing for the assessment of the structural capacity of the structure. A new practical analysis approach is used that examines the seismic response of the structure by comparing drift capacities with a possible earthquake deformations envelope. Of crucial significance in maintaining the architectural design of such important Modernity structures, is to assess their overall capacity, minimizing the required repairs; thus, the importance of taking under consideration the true pushover curve of the structure is highlighted through this study.*

Introduction

Codes for new construction are appropriate for the design of new buildings with detailing provisions and pertinent structural system for good seismic performance having regular configuration, structural continuity, ductile detailing and appropriate material quality. In order to evaluate the performance of existing buildings that were designed prior to the introduction of the current seismic design procedures (mostly with unfavourable configuration and poor detailing), appropriate assessment codes for existing buildings may be utilised. In recognition of the great likelihood of damage of existing sub-standard buildings, Code standards for structural assessment and upgrading have been developed worldwide ((EN 1998:3, 2005), (ASCE/SEI 41-17, 2017), (Japan Concrete Institute, 2014), (fib Bulletin No. 24, 2003), (NZSEE, 2017), (FEMA 273, 1997), (FEMA P154, 2015), (ASCE/SEI 31-03, 2004).

The level of performance to be chosen for historic structures varies according to individual case-by-case requirements and is selected by the overseeing stakeholder authority after consideration of several, occasionally conflicting criteria. For example, it could be mapped to the safety levels of normal buildings, or a higher level of performance could be chosen on account of the societal value of the monuments. Alternatively, a lower level of performance could be chosen in order to avoid damaging the historic fabric during retrofit, or higher performance objectives could be targeted for in order to enhance post-earthquake reparability (such categories defined by (ASCE/SEI 41-17, 2017) are: Enhanced Performance Objectives, Limited Performance Objectives, Basic-Performance Objective Equivalent to New Building Standards). Even though designated historic buildings are often afforded waivers or special considerations, this might not be appropriate in the case where public safety is of utmost importance and may thus be prioritized over and above the objectives of historic preservation; therefore the best fit solution should be somewhere between legislative restrictions regarding preservation of the historic construction and existing seismic codes (ASCE/SEI 41-17, 2017) with possible exceptions.

Modelling and structural assessment procedure in such cases is of outmost importance, as the capacity curve from the pushover analysis will determine the ductility demand of the structure and the corresponding level of damage that is likely to develop in a future seismic event.

[1] Researcher, Dep. of Civ. & Env. Eng., University of Cyprus, Nicosia, Cyprus, ageorg44@ucy.ac.cy
[2] Assoc. Prof., Dep. of Civil and Environmental Engineering, University of Cyprus, Cyprus
[3] Prof., Dep. of Civ. Eng., Lassonde Faculty of Engineering, York University, Canada

Analysis may be performed in 2-D frames or 3D models, if torsional response should be included. Design codes tend to become more sophisticated specifying 3-D modal analysis as a routine design tool. The advantage of this analysis is the improved representation of the higher modes of vibration with regards to static analysis, while its drawbacks are driving the design to unrealistic estimates of member stiffness, doubtful validity of results from modal combinations, under-estimation of drifts in lower stories and no consideration of the alteration of stiffness due to the axial force variation caused by the seismic axial load (Priestley, 2003).

Constructing the pushover curve in a structure with ductility deficiencies is not necessarily straightforward; two general approaches are followed, namely a force based and a displacement based procedure. In the case of force-based methods, which as a rule use the fundamental period and mode-shape in order to determine the distribution of forces through the structure, the use of elastic stiffness characteristics results to errors, which may even be worst in the case of inelastic response analysis (Priestley, 2003). With regards to stiffness calculations, most of the codes take into consideration the early cracking introduced by the seismic excitation by generally reducing the gross stiffness by 50%, while others use different adjustment factors for different member types or determine the cracked *EI* after calculation of the moment-curvature diagram of the members (KANEPE, 2017; NZSEE, 2017). In the case of the non-linear static (pushover) analysis, Eurocode 8 (EN 1998:3, 2005) requires the use of at least two lateral load pattern distributions (heightwise uniform and one varying with increasing distance from the ground according with the pattern of the fundamental mode). The lateral forces are applied at the location of mass in the model. The model is loaded with vertical (G+0.3Q) and increasing lateral loads and the capacity curve is determined. The elastic spectrum is then used to derive the target displacement (Informative Annex B, (EN1998-1-2004, 2004)).

Force-based analysis methods usually fail to provide solutions where realistic levels of displacements are attained due to convergence issues (modes of failure other than flexural create post-peak softening), or lead to unrealistic strength and deformation capacity estimates (Thermou, 2014). In this paper a force-based analysis of a historical building is compared with a simple displacement-based analysis proposed by Thermou (2014), considering also the coupled torsional effects in the first mode shape. The pushover curves are then compared with the Target Displacement provided by the seismic response spectra to evaluate the performance of the structure for the design intensity and the level of retrofit required for each case.

Case study description

Figure 1. Front (west) and side (north) elevation of the Old Municipality Market, Nicosia.

Historical Background

The Old Municipality Market (Fig. 1) was built in Nicosia, within the walled city, in 1967. It is a very important landmark building and a pure sample of the Modernism Architecture in Cyprus, designed by the known modernist architect S. Oikonomou. It was built after division of the walled city of Nicosia in 1964, as the original municipal market was located in the north side of the division line; therefore the need for a new municipality market was urgent. Due to its architectural value, its importance for the economy of the area and being a landmark building of the history of Cyprus, the Old Municipal Market was listed in 2011. At this moment, the building is undergoing restoration to be converted into a research center; hence, various investigations of its state are taking place.

Note that the Republic of Cyprus, which was only established in 1960, had no universities or centres until about 25 years ago and no regulations for design of concrete structures existed in

the past. Cypriot engineers who studied in various countries abroad were designing according to the regulations of those countries. There was no knowledge of the design practices against seismic excitations and no measurements of the local intensities of earthquakes, and therefore buildings were designed only for gravity loads. At that time, it is also important to note that there were no batching plants in Cyprus either and concrete was thus prepared on site in small quantities of 2 tn at a time. This led to great variability in the quality of concrete in the various parts of a structure, even from the bottom to the top of a column, as there was also no equipment for vibration and proper compaction and consolidation.

Visual Inspection

The building consists of four statically independent parts, separated with construction joints (3 cm). One part has a basement, but the rest of the structure has two floors above ground. Only the west part of the structure was selected for analysis in this study, as shown in Figure 2. Cracks are visible in most of the beams of the structure (Fig. 3(a)). Drainage from the roof passes through some of the external columns of the building (K11, K116, K115, K114, K113, K112). Most frames in the perimeter of the building have brick infill walls that do not extend to the full column height, thus creating captive columns. As shown in Fig. 3 (d) the base of the columns with drainage systems shows extensive concrete cracking, probably due to the corrosion of the reinforcement.

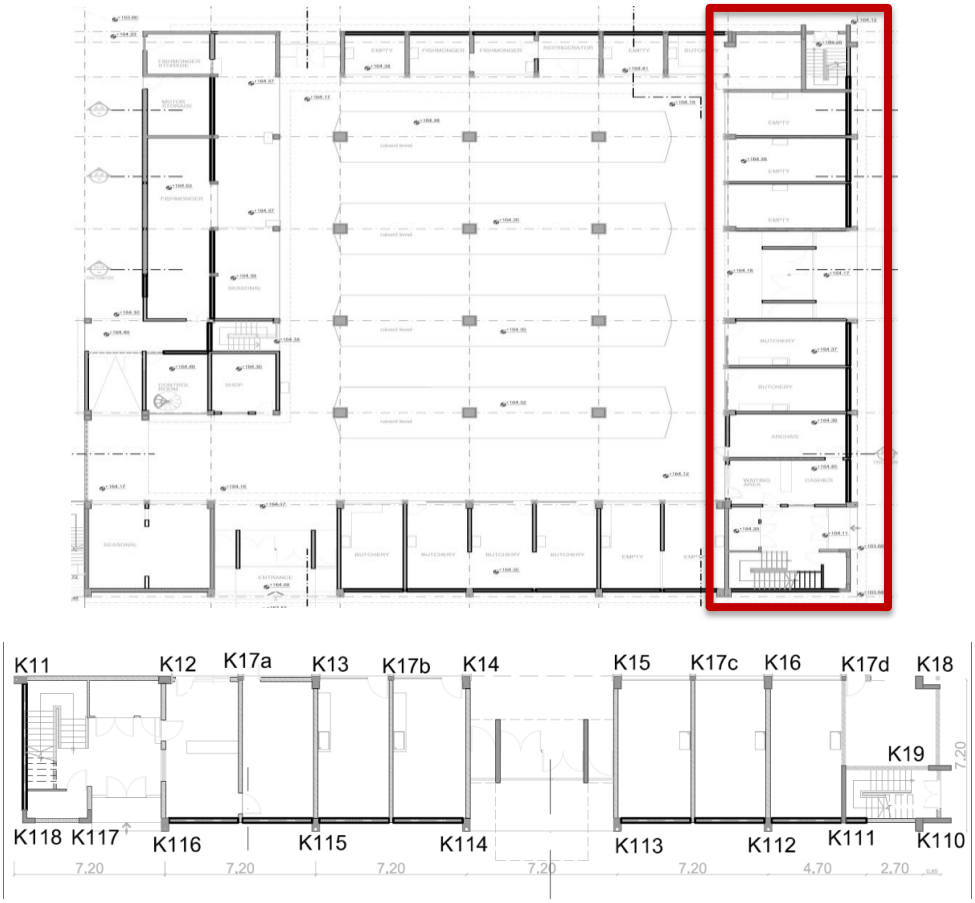

Figure 2. First floor and denomination of frame members.

Material Testing

The concrete mix design, as described on the old drawings that were found, is 1:1.5:3 by volume (cement:sand:coarse aggregates) for columns K1-K14 and 1:2:4 by volume for the rest of the structure. For the case of 1:2:4 analogies, based on verbal record, 1 part of water was used if the aggregates were wet, while 1.5-2 parts of water were used if the aggregates were dry. Various destructive and non-destructive tests were used to determine the materials' quality, including core extraction for compressive stress testing, depth of carbonation testing, chloride/sulfate concentration measurements, electrical resistivity measurements, use of cover meter for the verification of the reinforcement detailing, based on the old drawings that were

found. For the concrete mix, crushed diabase coarse aggregates and natural sand were used. An average of 22.3 MPa was found from the compression tests (EN 12504-1:2009) on the ground floor columns, with a standard deviation of 5.9 MPa, while in the north and west part columns, the compressive strength was in the order of 7 MPa. The mean compressive strength of the columns on the first floor was 22.3 MPa. Beams and floor slabs had higher compressive strengths and lower standard deviations. The carbonation depth (EN 14630:2006) was found to surpass the cover depth in most of the beams and columns. Reinforcement was 220 MPa mild steel without ribs.

Figure 3. (a) Crack locations in beams, (b) Column base with cast-in drainage pipe, (c) Short columns due to infill brick walls, and (d) Deterioration of concrete.

Structural System

The west side of the structure consists of R/C frame beams and columns with three walls located on one side of the plan, indicating that the center of rotation will be offset from the center of mass. Most of the columns and walls continue with the same dimensions in the 1st floor, except K12 whose dimensions are reduced from 1100x200 (mm) to 600x200(mm). Columns K17a-d are not continued to the 1st floor. Based on the old drawings of the structure that were found, column concrete cover was specified at 5 cm, while lap splices were 40d_b long. Beams' cross sectional width was varied from 0.2 m to 0.515 m, while the beam height was 0.7 m. The ground floor had a height of 4.45 m and the first floor of 3.10 m. The floor slabs were 0.2 m deep.

Table 1 lists dimensions, longitudinal and transverse reinforcement and the axial load from the G+0.3Q combination (EN 1998:3, 2005) and axial load ratio $v=N_{G+0.3Q}/(A_c f_c)$ for the first floor columns. Note that the front exterior columns are subjected to a value of v that is close to the limit of 0.4 that corresponds to balanced column failure, which identifies the limit of brittle response in the Axial – Load vs. Moment Interaction Diagram. This load ratio is estimated from service life loads only, without considering the additional axial load that the seismic overturning action will impose to the columns. On account of the high value of v along and the reported corrosion of reinforcement in the base of those columns, it is concluded that no moment can be resisted in their base; thus a hinge was assigned in the model.

Member	h_x	h_y	longitudinal	stirrups	N (kN)	v
K11	600	350	6Φ20	2Φ8/25	315	0.214
K12	600	350	6Φ20	2Φ8/25	524	0.356
K13 - K16	350	600	6Φ24	2Φ8/30	500	0.340
K17	200	200	4Φ12	Φ6/30	91	0.039
K19	1100	200	8Φ24+2Φ12	3Φ8/20	165	0.107
K18	600*350x1150*200		6Φ24xΦ12/25	2Φ8/25xΦ8/25	474	0.204
K110	600*350x1700*200		6Φ24xΦ12/25	2Φ8/25xΦ8/25	400	0.172
K111	200	2700	Φ12/20	Φ8/20	526	0.139
K112 - K116	350	600	6Φ24	2Φ8/30	577	0.393
K117	200*600x200*600		8Φ16	2Φ8/25	217	0.129
K118	200*600x200*600		8Φ20	2Φ8/20	378	0.225

Table 1. Ground floor columns characteristics.

Simulation of the structure in SAP2000

Member properties

The structure was modelled in the commercial software SAP2000 (CSI, 2009) in order to emulate standard assessment practice. The slabs were modelled using Plate-Thin elements with a thickness of 0.2 m, whereas the beams, columns and walls were simulated as frame elements. The walls were connected to the floor beams with rigid frame members having a depth equal to the floor height, which according to previous research (Kubin, Fahjan and Tan, 2008; Fahjan, Kubin and Tan, 2010) can better simulate reality. Moment-curvature diagrams based on the dimensions and reinforcement for all members were calculated using RESPONSE2000 (Bentz, 2000). Beam cross sections were considered to function as T sections for both sagging and hogging moments, also taking into consideration the slab reinforcement within the effective slab width. Slab reinforcement oriented parallel to a beam's axis may increase the flexural strength of the beam and increase the shear strength demand, which can cause premature web shear failure due to low shear reinforcement (KANEPE, 2017). The reduced stiffness of the members due to cracking was determined as $K_{b,c}=12EI/h^3$ for members fixed at both ends, and $K_w=3EI/h^3$ for members fixed at one end and pinned at the other, where EI was deduced from the moment-curvature diagrams from the ratio of the values at yielding: $EI=M_y/\varphi_y$. The stiffness of the frames was then accordingly reduced in the model by applying a reduction factor on the moments of inertia in the two directions. The nodes on the floors were assigned diaphragmatic restrains and additional nodes were assigned to the center of gravity of the floor slab in each storey.

	Y-Direction				X-Direction			
Member	**θ_y (%)**	**θ_u (%)**	**M_y**	**M_u**	**θ_y (%)**	**θ_u (%)**	**M_y**	**M_u**
K11	0.47	12.10	81.65	97.46	0.40	5.46	150	162
K12	0.62	9.14	99	101	0.30	1.04	159	170
K13-K16	0.30	1.04	186	199	0.62	8.53	116	123
K17	1.20	6.12	10.61	11.24	1.20	5.94	11	11
K19	1.06	20.51	57.55	71.161	0.24	3.61	359	442
K18	0.33	6.23	214.86	275.77	0.44	2.61	349	391
K110	0.28	5.65	206.239	277.62	0.08	1.61	472	660
K111	0.06	2.15	1145.2	1380.196	0.62	23.79	75	95
K112-K116	0.66	12.06	378	400.54	1.25	9.09	238	242
K117	0.15	5.60	76.97	112.24	0.15	4.93	77	112
K118	0.23	6.78	108.17	143.7	0.23	5.97	108	144

Table 2. Moment-Drift member properties for ground floor columns. (Moments in kN-m)

The M-φ curves extracted from RESPONSE2000 for all members were transformed into M-θ curves in order to be used in the hinge properties of the linear elements that were deployed for the simulation. The equations used for the transformation are as follows:

$$\theta_y = \frac{\varphi_y \cdot L_s}{3}\ ,\ \theta_{pl} = \left(\varphi_u - \varphi_y\right) \cdot l_{pl}\ ,\ \theta_u = \theta_y + \theta_{pl} \quad (1)$$

In Eqn. (1), L_s is the shear span of the members and l_{pl} is the length of the plastic hinge calculated as per EN 1998:3 (2005) for old-type members without seismic detailing as:

$$L_{pl} = 0.025L_s + 0.125h + 0.1d_b \cdot f_y \quad (2)$$

Table 2 lists key values of the M-θ curves for the columns in the ground floor in the X and Y axes.

Fundamental Periods and Mode Shapes

The 1st (fundamental) period was a translational mode in the y-axis with a period of T_1=0.911 sec (Fig. 4(a)), and 60% mass participation, the 2nd mode was also translational in the x-axis with a period of T_2=0.77 sec (Fig. 4(b)) with 93% of translational mass participation, while T_3=0.4 sec (Fig. 4(c)), with an additional 33% of the mass participating in y-axis translation (Table 3).

In order to determine the distribution of forces or displacements imported in the pushover analysis, the translations of the centers of mass and of all nodes at the top of the columns were recorded for the two primary mode-shapes in the x and y directions and the resulting normalized

vectors are, Φ_1=[0.7,1] and Φ_2=[0.67,1]. For the force-controlled pushover the distribution of lateral forces acting on the masses of each floor are computed EC8-Part 1 (Par. 4.3.3.2.3) as:

$$F_i = \frac{\varphi_i \cdot m_i}{\sum \varphi_j \cdot m_j} \quad (3)$$

where φ_i and φ_j are the displacement in the fundamental mode shape and m_i, m_j are the masses from the G+0.3Q load combination. The force distribution on the floor masses of the first and second floors was [371,629] in kN in the Y-direction and [307,693] in the X-direction.

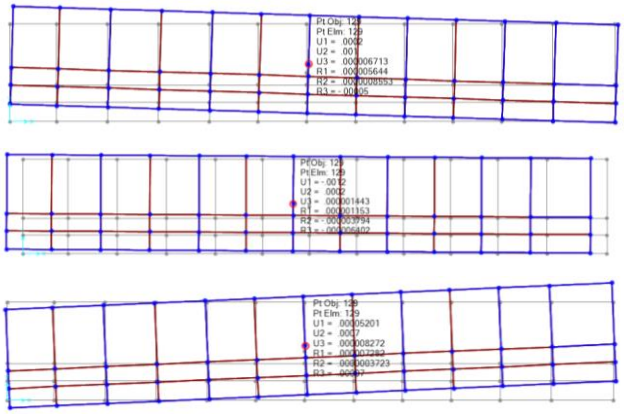

Figure 4. (a) 1st mode shape, (b) 2nd mode shape, (c) 3rd mode shape.

StepNum	Period T (sec)	MU_X	MU_Y	$SumMU_X$	$SumMU_Y$
1	0.911102	0.02913	0.6	0.02913	0.6
2	0.772658	0.93	0.02592	0.96	0.63
3	0.492586	0.001297	0.33	0.97	0.96

Table 3. Modal Participation Mass Ratios.

Rapid seismic assessment

Buildings constructed prior to the establishment of modern codes and design practices have been recognised to suffer from strong beam - weak column mechanisms, leading to plastic hinge localization in the columns instead of the beams and therefore the formation of a mechanism in the weakest floor of the structure and subsequently brittle collapse. Additionally, the limited shear reinforcement of columns, as well as the short anchorage and lap splice lengths, the lack of ribs of the reinforcement and the low concrete strength may lead to brittle anchorage, lap-splice, beam-columns joint, compressive strut brittle failures even prior to the yielding of the flexural reinforcement (Syntzirma and Pantazopoulou, 2007). The strength of each column may be estimated as the minimum shear required to enact any of the possible column failure mechanisms as per (Pardalopoulos, Pantazopoulou and Lekidis, 2018):

$$V_{fail}=min\ (V_{flex},\ V_v,\ V_j,\ V_{by}) \quad (4)$$

Where V_{flex} is the column shear for flexural yielding and failure equal to $M_{y\ or\ u}/L_s$, while the values of $M_{y\ or\ u}$ were extracted from fiber analysis through RESPONSE2000, V_v is the column shear strength determined from the compressive strut failure as:

$$if\ v \geq 0.1; V_v = v \cdot tana \cdot b \cdot d \cdot f_c + A_{tr} \cdot f_{st} \cdot \frac{d\cdot(1-\xi)}{s} \cdot cot\theta_v \quad (5)$$

$$if\ < 0.1; V_v = A_{tr} \cdot f_{st} \cdot \frac{d\cdot(1-\xi)}{s} \cdot cot\theta_v \quad (6)$$

Where $tan\ \alpha=(h/d\ -0.8\cdot\xi)\cdot d/h_{cl}$, α is the angle of inclination of the diagonal strut that is defined by the line connecting the centroid of the compression zones in the opposite sections of a column. Note that $\alpha \leq \theta_v$, with θ_v being the angle of the slidding failure plane. θ_v equals 45° when v < 0.10 and 30° when v≥0.25, whereas linear interpolation is used for intermediate values of the axial load ratio, v; θ_v is measured with reference to the longitudinal axis and it determines the number of stirrup legs that are intersected by the inclined sliding plane. Additionally the column shear at joint failure for unreinforced or lightly reinforced joints is calculated by:

$$V_j = \gamma_j \cdot 0.5 \cdot \sqrt{f_c} \cdot \sqrt{1 + \frac{\nu_j \cdot f_c}{0.5 \cdot \sqrt{f_c}} \frac{b_j \cdot d \cdot d_b}{h_{col}}} \quad (7)$$

With γ_j ={1.40 for interior joints; 1.00 for all other cases}, ν_j is the (service) axial load acting on the bottom of the column adjusted at the top of the joint (compression positive), d_{beam} is the beam depth and $b_j = (b+b_{beam})/2$ is the joint width. The above procedure was performed for all the columns of the ground floor (GF) and first floor (FF) of the building and results of the GF for both directions are depicted in Fig. 5.

For each individual member the failure shear based on all possible mechanisms was implemented as the ultimate moment or shear to be employed both for the non-linear F.E. simulation and for the displacement control approach delivered by spreadsheet. The failure mechanisms and *V-θ* curves' characteristic points for each column are listed in Table 4.

The final V-θ characteristic points for each member were used to define the hinge properties in the non-linear analysis with SAP2000. Hinges were deformation controlled with ductile behavior, using the Interacting M2-M3 option, doubly symmetric about the two axes of the cross section.

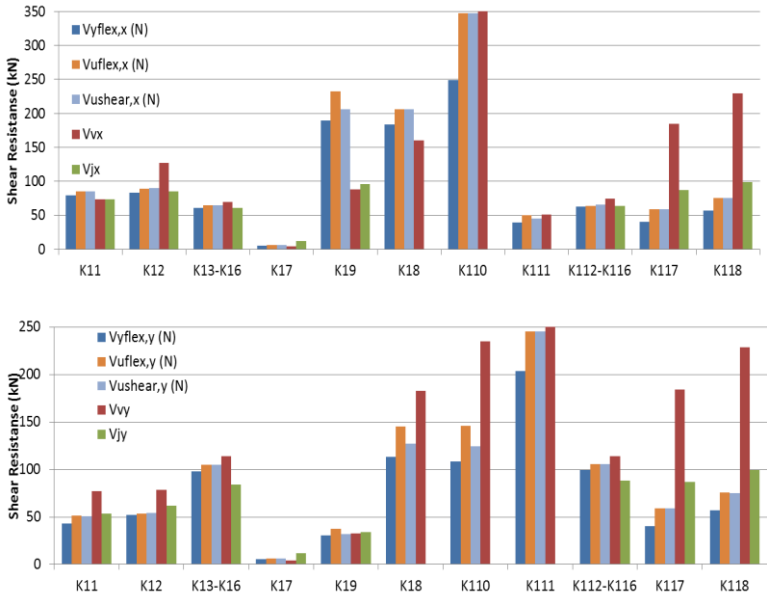

Figure 5. Failure mechanisms of members in X-direction (top) and Y-direction (bottom).

	Y-direction					X-direction				
Member	**V_{yflex} (kN)**	**V_{fail}**		**θ_y (%)**	**θ_u (%)**	**V_{yflex} (kN)**	**V_{fail}**		**θ_y (%)**	**θ_u (%)**
K11	43.0	50.5	shear	0.47	10.99	73.4	73.4	joint	0.37	0.37
K12	52.1	53.2	flexure	0.62	9.14	83.47	85.4	joint	0.30	0.54
K13-K16	84.1	84.1	joint	0.26	0.26	61.05	61.2	joint	0.62	0.86
K17	4.4	4.4	strut	0.94	0.94	4.4	4.4	strut	0.94	0.94
K19	30.3	31.9	shear	1.06	5.43	87.9	87.9	strut	0.11	0.11
K18	113.1	127.5	shear	0.33	2.98	160.6	160.6	strut	0.39	0.39
K110	108.5	124.7	shear	0.28	2.59	248.58	347.0	shear	0.08	1.61
K111	203.6	245.4	flexure	0.06	2.15	39.47	45.1	shear	0.62	13.00
K112-K116	88.2	88.2	joint	0.59	0.59	62.63	63.7	flexure	1.25	9.09
K117	40.5	59.1	flexure	0.15	5.60	40.51	59.1	flexure	0.15	4.93
K118	56.9	75.3	shear	0.23	6.67	56.93	75.3	shear	0.23	5.87

Table 4. Failure mechanisms of GF members and V-θ characteristic points.

Results from the analysis

Displacement controlled analysis

Recent studies (Thermou, 2014) have shown that by using a displacement based approach instead of a lateral load pattern of increasing intensity can increase the validity of the prediction

of failure of structures as it does not require a positive-definite stiffness matrix for convergence. The pushover analysis resistance curve in this approach is obtained by applying a drift demand pattern based on the fundamental mode of translational vibration of the structure. The procedure of assessment proposed by (Thermou, Elnashai and Pantazopoulou, 2010) is adopted as follows:

1. A displacement of increasing magnitude Δ is applied at the top of the structure
2. Using the response shape Φ which was obtained from the modal analysis performed in SAP2000, for the 1st mode shape and for the 2nd mode shape, the distribution of displacements is given for each floor ($\Delta_j=\Delta\cdot\Phi_j$) and the inter-storey drift ratio is computed $IDj=\Delta\cdot(\Phi_j-\Phi_{j-1})$
3. The inter-storey drift ratio is distributed to beams and columns, i.e. for columns the rotation demand is $\theta_c=\lambda/(\lambda+1)\cdot\theta_{bc}$, based on the relative stiffness between the members $\lambda=EI_b\cdot h_c/(EI_b\cdot h_c)$, where λ is corrected for each next step, taken as 1 if the member (column) has passed its yield point
4. The base shear is estimated based on the response curve of the first floor given the estimated drift demands for the first floor columns using the steps 1-3 above.

The pushover curves were determined both with and without consideration of the *P-Δ* effects, by reducing the ultimate moment and drift available to be undertaken by the members:

$$V_{fp-d} = V_{fail} - N_{g+0.3q}\cdot\theta_u \tag{8}$$

It was found that due to the brittle failures of most of the members prior or soon after yielding of flexural reinforcement, the P-Δ effect was not high enough to affect the pushover curve of the structure in both directions. Progression of failures from the Displacement control method is shown in Figure 6 for both directions, where yielding is denoted in yellow and failure in red colour.

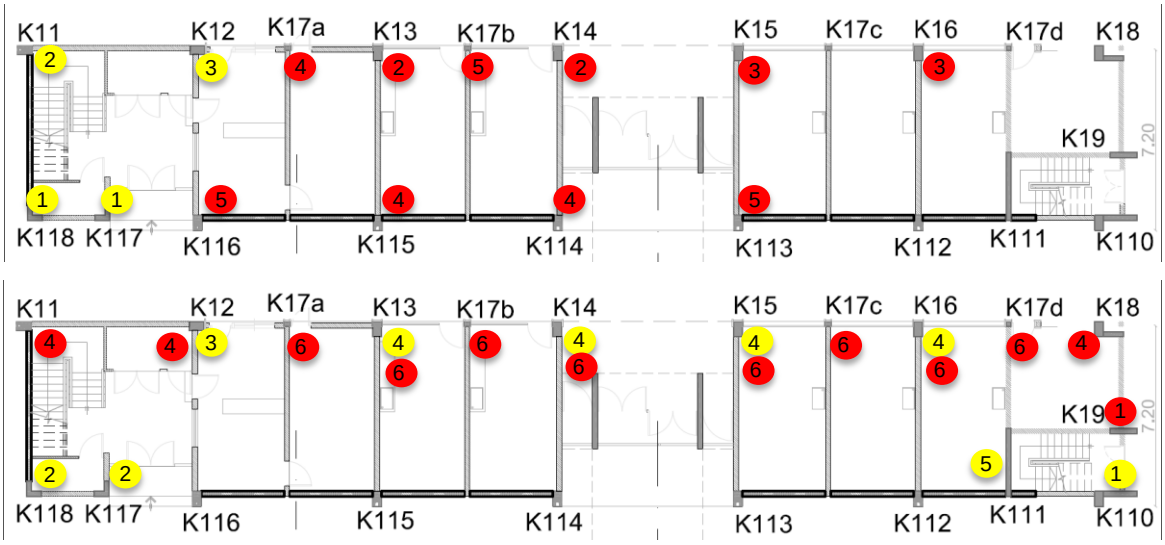

Figure 6. Displacement control pushover progressive failures in Y (top) and X-directions (below)

Load controlled Pushover Y-direction

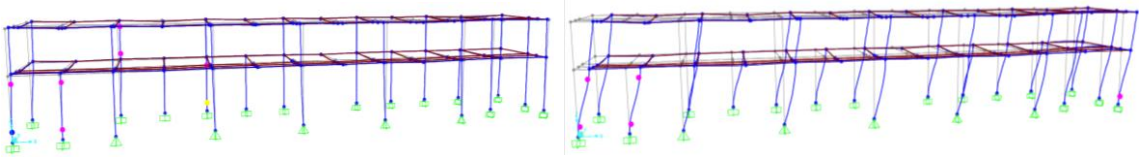

Figure 7. Force-controlled pushover progressive failures in Y-direction (top) and X-direction (bottom) (pink-yield point, yellow-ultimate).

SAP2000 was used to perform a non-linear analysis in the two directions with increasing lateral loads applied at the center of masses of each floor. The type of the analysis was static nonlinear with geometric nonlinearities taking into account P-Delta effects. The analysis in both

directions stopped due to convergence issues. Figure 7 shows the state of plastic hinges at the final stage at which the analysis was inadvertedly terminated in both directions.

Comparison of load-control and displacement-control pushover curves

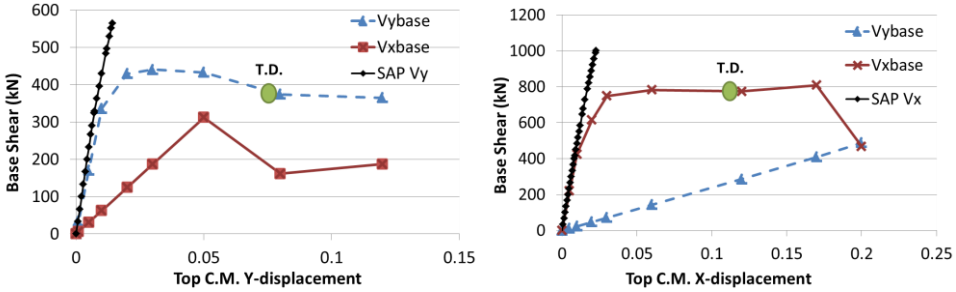

Figure 8. Pushover curves of force-controlled and displacement-controlled methods in (a) Y-direction and (b) X-direction.

Figure 8 shows the Base Shear versus top node displacement at the center of mass in the Y-axis and X-axis, when either load or displacement patterns are applied in order to conduct the pushover analysis in the respective direction. Additionally to the Base Shear in the same direction of the loading, in the case of the displacement-controlled analysis the base shear in the perpendicular direction is displayed; this appears due to the eccentricity of the center of mass from the center of rotation. Even though both procedures seem to give the same initial stiffness of the structure prior to yielding, the force-controlled approach does not assess the plastic deformations and ductility displayed by the structure. By using the Type I design response spectrum for Cyprus, Nicosia (0.2g), for Soil Type C (S=1.15, T_B=0.2 sec, T_c=0.6 sec), the procedure described in Annex B of Eurocode 8:Part 3 (BS EN 1998:3, 2005) is used to determine the target displacement and thereafter the need for seismic upgrading of the structure based on the two different approaches used. This procedure is summarized below:

Using the identified mode-shapes the system was first transformed to an equivalent Single Degree of Freedom (SDOF) system by computing its mass as $m^*=\Sigma m_i \cdot \Phi_i$, $m_y^*=689$ *tn* and $m_x^*=662$ *tn*. The mode participation factor $\Gamma = m^*/(\Sigma m_i \cdot \Phi_i^2)$ was calculated as: $\Gamma_y=1.17$ and $\Gamma_x=1.2$. The idealized elasto-perfectly plastic force-displacement relationship was then determined (milestone points with coordinates F_y^*, d_m^*, d_y^*), as well as the period T^* of the idealized equivalent SDOF system by $T^*=2\pi(m^* d_y^*/ F_y^*)^{1/2}$ were calculated as listed in Table 5. The target displacement of the structure was computed from the elastic acceleration response spectrum at the period of T^*. For the range of periods of interest, the elastic spectrum acceleration was $S_e(T^*)=a_g \cdot S \cdot \eta \cdot 2.5(T_o/T^*)$, where n is the damping correction factor equal to 1, whereas the corresponding SDOF displacement was $d_t^* = S_e(T^*)(T^*/2\pi)^2$. Finally the MDOF displacement was computed as $d_t=\Gamma \cdot d_t^*$.

	Displacement-controlled		Force-controlled	
	Y	X	Y	X
F_y^*=	377576	674690.6	483495	856942
d_m^*=	0.026	0.142	0.012	0.019
d_y^*=	0.008	0.021	0.010	0.018
T^*=	0.771	0.906	0.766	0.732
d_t=	0.079	0.095	0.078	0.077

Table 5. Displacement demand for displacement and force-controlled approach.

Table 5 shows the Target Displacements (T.D.) that will be requested at a possible future seismic event by the structure having an intensity that is comparable to that of the design ground acceleration value for the site of interest. Note that the estimated required displacements of the structure for the expected seismic excitation are very closely estimated regardless of the assessment method used for the analysis.

Conclusions

This study focuses on the seismic assessment of a concrete heritage structure with brittle details. The paper summarizes information for the specific structure, the available materials,

and the local construction practices in the 1960's in Cyprus, with the intent that this case study may be used as a guide for the evaluation of concrete structures that were built in that period in the island. The assessment is performed by a force controlled (program based) and a displacement controlled (by spreadsheet) push-over analysis. The procedure shows that the force based analysis (of demand vs. capacity) will significantly overestimate the demands for seismic upgrading, whereas the displacement control approach shows that Target Displacements are within the capabilities of the structure, with possible restoration requirements only to diminish any forms of brittle failures of the members.

Acknowledgements

The authors would like to thank Nicosia Master Plan for providing records and test results for the structure under study. Structural assessment of the building is part of the JPI Cultural Heritage research program CONSECH20, co-funded by the Republic of Cyprus through the Cyprus Research Promotion Foundation (Project P2P/JPICH_HCE/0917/0012).

References

ASCE/SEI 31-03 (2004) ASCE 31-03: Seismic Evaluation of Existing Buildings. ASCE. doi: 10.1061/40700(2004)75.

ASCE/SEI 41-17 (2017) Seismic Evaluation and Retrofit of Existing Buildings, Reston, Virginia. doi: 10.1061/9780784414859.

Bentz, E. C. (2000) Sectional Analysis of RC Members. University of Toronto, Canada.

CSI (2009) 'SAP2000: v. 14.0'. Berkeley, California: Computers and Structures, Inc.

EN 1998:3 (2005) Assessment and retrofitting of buildings. Brussels: CEN/CENELEC Internal Regulations.

EN1998-1-2004 (2004) Eurocode 8. Design of structures for earthquake resistance—Part 1: general rules, seismic actions and rules for buildings. Brussels.

Fahjan, Y. M., Kubin, J. and Tan, M. (2010) 'Nonlinear Analysis Methods for Reinforced Concrete Buildings with Shear walls', Proc., 14th ECEE.

FEMA 273 (1997) NEHRP GUIDELINES FOR THE SEISMIC REHABILITATION OF BUILDINGS. Washington, D.C.: BUILDING SEISMIC SAFETY COUNCIL.

FEMA P154 (2015) Rapid Visual Screening of Buildings for Potential Seismic Hazards: A Handbook. 3rd edn, Disaster Prevention and Management: An Intnl. J. Edited by ATC. Wash., D.C. : FEMA, doi: 10.1108/dpm.2003.07312dab.015.

fib Bulletin No. 24 (2003) Seismic Assessment & retrofit of RC buildings. fib Task Group 7.1 Assessm./retrofit of existing structures. Laus., Switzerl.: Intnl. Fed. for Struct. Concr. (fib).

Japan Concrete Institute (2014) 'Guidelines for Assessment of Existing Concrete Structures'. Tokyo, p. 70.

KANEPE (2017) Greek Retrofitting Code. Edited by Greek Organisation for Seismic Planning and Protection (OASP). Athens, Greece: Greek Ministry for Envir. Plan. & Public Works.

Kubin, J., Fahjan, Y. M. and Tan, M. T. (2008) 'Comparison of Practical Approaches for Modelling Shearwalls in Structural Analyses of Buildings', 14th WCEE, (1988).

NZSEE (2017) The Seismic Assessment of Existing Buildings. 1st edn. Edited by R. Jury. New Zealand: Ministry of Business, Innovation and Employment, Earthquake Commission.

Pardalopoulos, S. I., Pantazopoulou, S. J. and Lekidis, V. A. (2018) 'Simplified method for rapid seismic assessment of older R . C . buildings', Engin. Struct. Elsevier, 154(Jan.):10–22.

Priestley, M. J. N. (2003) Myths and Fallacies in Earthquake Engineering, Revisited, The Ninth Mallet - Milne Lecture. Pavia Italy: Rose School.

Syntzirma, D. V. and Pantazopoulou, S. J. (2007) 'Deformation capacity of r.c. members with brittle details under cyclic loads', ACI SP. 236, ACI-ASCE C(Seismic Shear).

Thermou, G. E. (2011) 'Comparative evaluation of Displacement-based vs . Force-based pushover analysis of seismically deficient R. C. structures.', Proc. of the 8th International Conference on Structural Dynamics, EURODYN 2011, Leuven, Belgium

Thermou, G. E., Elnashai, A. S. and Pantazopoulou, S. J. (2010) 'Design and assessment spectra for retrofitting of RC buildings', J. Earthq. Engrg., 14(5), pp. 743–770.